

## *In situ* monitoring of enzyme-catalyzed (co)polymerizations by Raman spectroscopy†‡

Matthew T. Hunley,<sup>a</sup> Atul S. Bhangale,<sup>ab</sup> Santanu Kundu,<sup>a</sup> Peter M. Johnson,<sup>a</sup> Michael S. Waters,<sup>a</sup> Richard A. Gross<sup>\*b</sup> and Kathryn L. Beers<sup>\*a</sup>

Received 29th September 2011, Accepted 10th November 2011

DOI: 10.1039/c1py00447f

*In situ*, fiber optic-based Raman spectroscopy provided real time monitoring of enzyme-catalyzed ring-opening homo- and copolymerizations of  $\epsilon$ -caprolactone ( $\epsilon$ -CL) and  $\delta$ -valerolactone ( $\delta$ -VL). A custom designed reactor equipped with *in situ* fiber optic probe was used to measure monomer conversion as a function of time. The results from the *in situ* technique were in good agreement with those determined by offline <sup>1</sup>H NMR analysis. Monomer reactivity ratios for the lipase-catalyzed copolymerization of  $\epsilon$ -CL and  $\delta$ -VL were estimated using the Kelen-Tudos method as  $r_{\epsilon\text{-CL}} = 0.38$  and  $r_{\delta\text{-VL}} = 0.29$ .

Rapidly growing interest in renewable and sustainable polymers is driving the development of novel catalyst systems for the ring-opening polymerization (ROP) of cyclic esters and carbonates.<sup>1–4</sup> Traditionally, metal catalysts such as tin 2-ethylhexanoate or titanium *tert*-butoxide have efficiently catalyzed ROP of lactones and lactides,<sup>5</sup> but recent reports have demonstrated the efficacy of less toxic metal catalysts<sup>1</sup> (based on aluminum, zinc, and magnesium, among others) as well as organocatalysts,<sup>2</sup> which eliminate the need for heavy metals. Recently, enzymes have been discovered which perform similarly to metal catalysts.<sup>4</sup> In comparison to traditional metal catalysts, immobilized enzyme-catalyzed reactions have several advantages: heavy metal-free synthesis, high selectivity, milder operating conditions, simple catalyst removal, and the production of enzymes from renewable sources. A major limitation for enzyme-catalyzed reactions is the need for better control necessary to supplant metal catalysis routes, although limited knowledge about reaction

kinetics hinders the ability to make substantial improvements to the process.

Ring-opening copolymerizations of many lactone systems have been studied to tailor degradation rates, improve thermal properties, and enhance mechanical and barrier properties.<sup>6–9</sup> However, many reports describe the formation of “blocky” copolymers,<sup>9,10</sup> and transesterification reactions can interrupt the stereoregularity and compositional architecture of the copolymers.<sup>10</sup> In addition, very few manuscripts report monomer reactivity ratios to describe the copolymerization behavior. Traditional offline analysis techniques such as nuclear magnetic resonance (NMR) spectroscopy and gas chromatography (GC) can provide accurate measures of monomer conversion, polymer compositions, and monomer sequence distributions, but are time consuming and require removing aliquots from the reaction. The determination of reactivity ratios conventionally depends on low-conversion analysis of monomer consumption where sampling times are highly important. Furthermore, for moisture- or photo-sensitive reactions, removal and storage of reaction aliquots may cause undesirable side reactions. Additional problems such as changes in reaction volume, especially with solid-supported catalysts, and difficulties in withdrawing uniform aliquots from heterogeneous systems further support the need for non-invasive, *in situ* monitoring techniques. Online spectroscopic tools such as FTIR and Raman spectroscopy have been demonstrated as effective tools to simultaneously monitor the copolymerization of two monomers for reactivity ratio determination.<sup>11,12</sup> Recent work by Schue and others verified that *in situ* Raman spectroscopy can reliably monitor the ROP of L-lactide and  $\epsilon$ -caprolactone.<sup>13,14</sup>

In an earlier effort, we used *in situ* NMR spectroscopy to investigate heterogeneous, immobilized enzyme-catalyzed polymerization reactions.<sup>15–17</sup> NMR spectroscopy suffers limited applicability to these systems due to mass transfer limitations that require continuous and controlled mixing. Furthermore, acquisition times to satisfy signal-to-noise requirements in NMR experiments can vary from seconds to minutes, leaving long periods between measurements. In comparison, Raman spectroscopy techniques have evolved as a promising tool for quantitative monitoring of chemical reactions *in situ* which require no reaction modifications and precise measurements of reaction kinetics in otherwise inaccessible conditions.<sup>11,18–21</sup> In this work, we demonstrate *in situ* Raman spectroscopy to investigate the kinetics of lactone homo- and copolymerization using immobilized lipase catalysis. Raman kinetic monitoring

<sup>a</sup>Polymers Division, National Institute of Standards and Technology, Gaithersburg, MD, 20899, USA. E-mail: beers@nist.gov; Fax: +1 (301) 975-4924; Tel: +1 (301) 975-2113

<sup>b</sup>Polytechnic Institute of NYU, Brooklyn, NY, 11201, USA. E-mail: rgross@poly.edu; Tel: +1 (718) 260-3024

† Electronic supplementary information (ESI) available: detailed description of materials and methods as well as Raman spectra. See DOI: 10.1039/c1py00447f

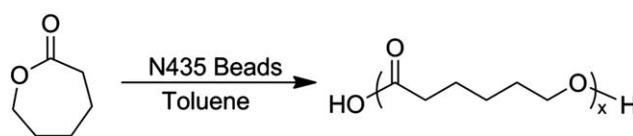
‡ Certain commercial equipment, instruments, or materials are identified in this paper in order to specify the experimental procedure adequately. Such identification is not intended to imply recommendation or endorsement by the National Institute of Standards and Technology, nor is it intended to imply that the materials or equipment identified are necessarily the best available for the purpose.

provided similar reaction kinetics as compared to *ex situ* techniques with the potential for real-time feedback of reaction kinetics. Since enzyme catalyzed ROP of polyesters have been traditionally studied in batch reactors,<sup>4,22</sup> only minor modifications are required to enable kinetic monitoring using Raman spectroscopy.

We designed an experimental system in which a fiber-optic Raman probe was incorporated within a batch reactor (Fig. 1). An aluminum heating block uniformly heated a 5-mL round bottom flask with feedback control while keeping the flask in contact with the external Raman probe (Further details of the setup as well as a full description of materials and methods are available in the Electronic Supplementary Information (ESI)). We selected the ROP of  $\epsilon$ -caprolactone ( $\epsilon$ -CL) to poly( $\epsilon$ -caprolactone) (PCL) as the model reaction due to the reactivity of  $\epsilon$ -CL under a wide range of conditions and its well-resolved ring-stretching peak in the Raman spectrum ( $696\text{ cm}^{-1}$ ). The polymerizations were conducted in toluene using the immobilized enzyme catalyst Novozyme 435 (N435)<sup>‡</sup> which consists of *Candida antarctica* Lipase B (CAL B) physically immobilized on a macroporous acrylate resin (Scheme 1). To obtain quantitative information on monomer conversion, a calibration curve was constructed using samples with known concentration of monomer and polymer (see Figure S1a in the ESI).

Fig. 2 shows the monomer conversion *versus* time for  $\epsilon$ -CL polymerizations at varying temperatures from  $25\text{ }^{\circ}\text{C}$  up to  $70\text{ }^{\circ}\text{C}$ . To validate that the *in situ* Raman spectroscopy method described above provides accurate values of monomer conversion, results obtained were compared to those measured by  $^1\text{H}$  NMR spectroscopy. For this purpose, aliquots were withdrawn from the reactions at times corresponding to large changes in  $\epsilon$ -CL conversion. The conversions calculated by Raman and  $^1\text{H}$  NMR agreed well within experimental error, validating that the *in situ* Raman spectroscopy method described here is accurate and consistent for characterization of enzyme-catalyzed ROP reactions over a wide range of temperatures. Furthermore, *in situ* Raman spectroscopy allows for more data points to be taken over the course of the reaction; we are restricted in the number of aliquots withdrawn from a reaction in order that the total reaction volume does not fall below 90% of the initial volume. Aliquots withdrawn leave the heterogeneous catalyst in the reaction media so that the catalyst concentration increases with the number of withdrawn samples.

The model copolymerization system consisted of  $\epsilon$ -CL and  $\delta$ -valerolactone ( $\delta$ -VL) (Scheme 2) due to the similar polymerization kinetics of both monomers using the CAL B enzyme as well as their well-resolved ring-stretching peaks in the Raman spectra ( $\epsilon$ -CL at  $696\text{ cm}^{-1}$  and  $\delta$ -VL at  $745\text{ cm}^{-1}$ ). The homopolymerizations of  $\epsilon$ -CL and  $\delta$ -VL are well studied,<sup>4</sup> and several reports have investigated the



**Scheme 1** Polymerization of  $\epsilon$ -CL to PCL by immobilized *Candida antarctica* lipase B (N435 beads).

copolymerizations of the two monomers by enzyme and metal catalysts.<sup>23–25</sup> Most catalysts yielded statistical sequence distributions in the copolymer products except for titanium(IV) butoxide, which resulted in copolymers with more blocky sequences after polymerization at  $260\text{ }^{\circ}\text{C}$ .<sup>24</sup> However, copolymer characterization relied on  $^1\text{H}$  and  $^{13}\text{C}$  NMR spectroscopy of products isolated after termination of the reaction. Homopolymerizations of  $\epsilon$ -CL and  $\delta$ -VL in the presence of N435 beads demonstrated that  $\epsilon$ -CL polymerizes faster than  $\delta$ -VL, as reported previously<sup>4</sup> (Figure S2 in the ESI). During copolymerization, the disappearance of both monomers was monitored simultaneously, as shown in Fig. 3. Consistent with homopolymerization rates,  $\epsilon$ -CL was consumed faster than  $\delta$ -VL during the copolymerization. Again,  $^1\text{H}$  NMR analysis confirmed the conversion trends observed by Raman spectroscopy. In both the homo- and copolymerizations with  $\delta$ -VL, a short induction period was observed before the monomer consumption began. Such behaviour has been observed previously for  $\delta$ -VL catalysed by both aluminium and enzyme catalysts.<sup>26,27</sup>

The differential form of the copolymer composition equation,

$$\frac{d[M_1]}{d[M_2]} = \frac{[M_1](r_1[M_1] + [M_2])}{[M_2]([M_1] + r_2[M_2])}, \quad (1)$$

correlates the reactivity ratios  $r_1$  and  $r_2$  to monomer concentrations  $[M_1]$  and  $[M_2]$  and the ratio of monomer disappearance rates

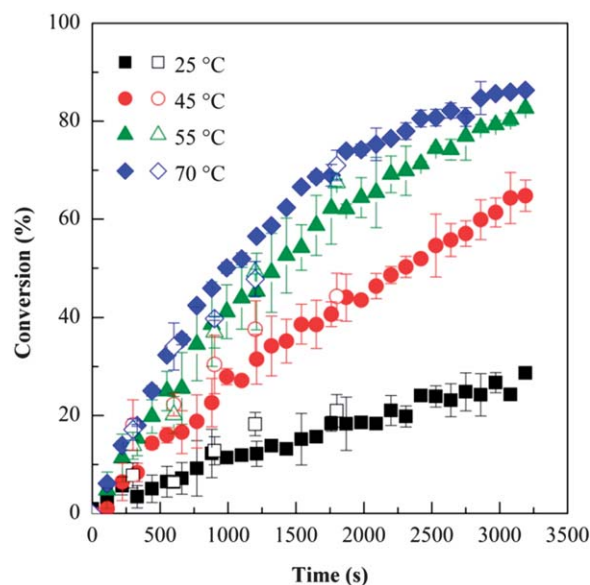


**Fig. 2** Conversion of  $\epsilon$ -CL as a function of reaction time for the enzyme-catalyzed ROP in toluene at different temperatures. Measurements of  $\epsilon$ -CL conversion by *in situ* Raman spectroscopy are designated with filled symbols whereas measurements of  $\epsilon$ -CL conversion by offline  $^1\text{H}$  NMR analysis are designated with non-filled symbols. The error bars indicate one standard uncertainty based on measurements on at least three different samples.

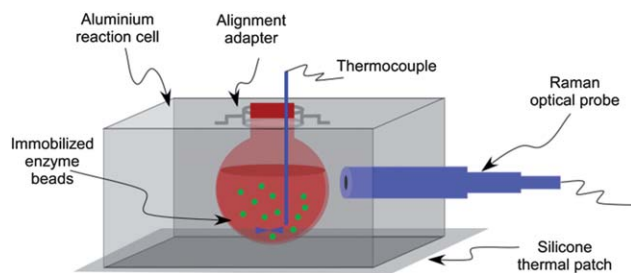
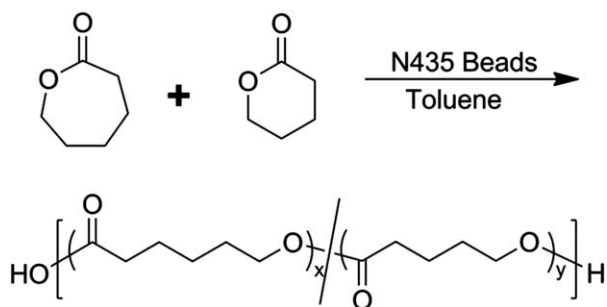


**Fig. 1** Reactor system constructed to monitor enzyme-catalyzed ROP of lactones by *in situ* Raman spectroscopy.



**Scheme 2** Copolymerization of  $\epsilon$ -CL and  $\delta$ -VL by immobilized *Candida antarctica* lipase B (N435 beads).

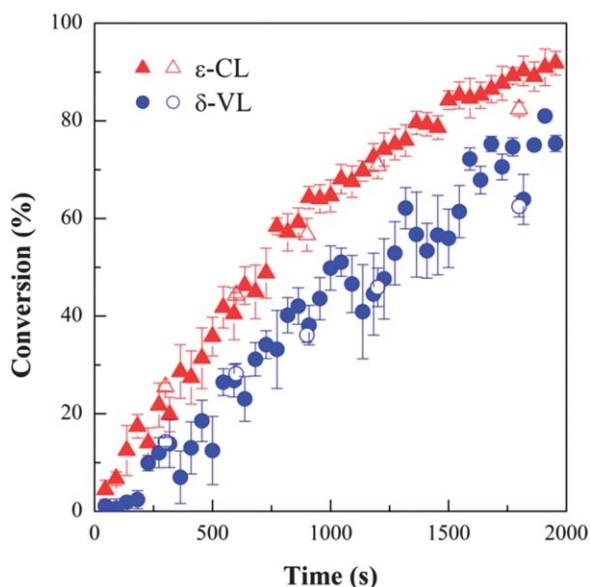


**Fig. 3** Conversion of  $\epsilon$ -CL and  $\delta$ -VL as a function of time for enzyme-catalyzed copolymerization with initial feed ratio  $[\epsilon\text{-CL}]/[\delta\text{-VL}] = 1$ . Conversion measurements by *in situ* Raman spectroscopy are designated with filled symbols whereas measurements by offline  $^1\text{H}$  NMR analysis are designated with non-filled symbols. Error bars indicate one standard uncertainty based on measurements on at least three different samples.

$d[M_1]/d[M_2]$ . The ratio of monomer disappearance,  $d[M_1]/d[M_2]$ , reflects the instantaneous copolymer composition at each time point during the reaction. Experimentally, the ratio of monomer disappearance can be measured at several different known monomer feed ratios to estimate the reactivity ratios. To simplify the determination of reactivity ratios, Fineman and Ross<sup>28</sup> rearranged the copolymer composition equation to the linear form

$$G = r_1 F - r_2, \quad (2)$$

where  $G = X(Y - 1)/Y$ ,  $F = X^2/Y$ ,  $X = [M_1]/[M_2]$ , and  $Y = d[M_1]/d[M_2]$  (the F-R model). Kelen and Tudos<sup>29</sup> refined this model as

$$\eta = \left[ r_1 + \frac{r_2}{\alpha} \right] \xi - \frac{r_2}{\alpha} \quad (3)$$

where  $\eta = G/(\alpha + F)$ ,  $\xi = F/(\alpha + F)$ , and  $\alpha = (F_{\min} F_{\max})^{1/2}$ , where  $F_{\min}$  and  $F_{\max}$  are the lowest and highest  $F$  values, respectively (the K-T

model). Linear regression of the plot of  $\eta$  versus  $\xi$  yields a line with the slope  $(r_1 + r_2/\alpha)$  and  $y$ -intercept  $-r_2/\alpha$ . The K-T refinement weights all data points equally, eliminating the problems of unequal weight inherent in the F-R model. In addition, to accurately reflect the initial monomer ratio of a copolymerization, the copolymer composition must be measured at low conversions ( $<5\%$ ) to limit the effect of compositional drift when one monomer is more reactive than the other.

Copolymerizations were performed at  $[\epsilon\text{-CL}]/[\delta\text{-VL}]$  ratios from 0.57 to 2.58 to monitor the copolymerization behavior. Using linear least-squares regression, the reactivity ratios were estimated as  $r_{\epsilon\text{-CL}} = 0.38 \pm 0.06$  and  $r_{\delta\text{-VL}} = 0.29 \pm 0.03$ . The plot of  $\eta$  versus  $\xi$  to determine reactivity ratios is shown in Figure S3 in the accompanying ESI. To better visualize the errors associated with these reactivity ratios, the 95% joint-confidence interval (JCI) ellipse was constructed as shown in Fig. 4a (the calculation of the JCI is described in detail in the ESI). The elliptical nature of the JCI has been observed previously for free radical and controlled radical copolymerizations.<sup>11,30</sup> To validate the reactivity ratio calculations, the copolymer compositions at low conversion ( $<10\%$ ) were determined by  $^1\text{H}$  NMR for a wide range of monomer feed ratios from 0.10 to 4.5. Fig. 4b plots the copolymer compositions versus monomer feed ratio along with the curve showing expected compositions based on the reactivity ratios calculated above and the copolymer composition equation,

$$F_1 = \frac{r_1 f_1^2 + f_1 f_2}{r_1 f_1^2 + 2 f_1 f_2 + r_2 f_2^2} \quad (4)$$

The experimental copolymer composition values agreed very well with the expected composition behavior, even at very high and very low  $\delta$ -VL concentrations. The reactivity ratios indicate a slight alternating behavior ( $r_{\epsilon\text{-CL}} < 1$  and  $r_{\delta\text{-VL}} < 1$ ), with each monomer preferring to cross-propagate. This behavior differs slightly from the enzyme-catalyzed copolymerization of  $\epsilon$ -CL and 1,5-dioxepan-2-one (DXO), which exhibited copolymerization behavior closer to the ideal case ( $r_{\epsilon\text{-CL}} = 0.9$  and  $r_{\text{DXO}} = 1.3$ ;  $r_{\epsilon\text{-CL}} \bullet r_{\text{DXO}} = 1.15$ ).<sup>31</sup>

Both the F-R and K-T models are derived from a terminal model of chain propagation, and the reactivity ratios describe the preference of a propagating chain to homopropagate or cross-propagate. The reactivity ratio is defined as the ratio of reaction rate constants for these two reactions,  $r_1 = k_{11}/k_{12}$ . In the case of enzyme-catalyzed ROP, the incorporation of monomer into the growing polymer chain involves two separate reactions: ring opening to form enzyme-activated monomer and reaction of enzyme-activated monomer with a propagating chain. In homopolymerizations, the ring-opening step is generally considered the rate limiting kinetic step because the propagating chain presumably reacts rapidly with the activated monomer.<sup>4</sup> The *in situ* Raman technique directly measures monomer consumption, which reflects the ring-opening kinetic step. The analysis of copolymer composition (Fig. 4b) agreed very well with the reactivity ratios by *in situ* Raman, confirming that the Raman analysis accurately reflects the copolymer composition. However, the propagation kinetics may differ significantly during copolymerization. The exact kinetic definition of the reactivity ratios for enzymatic ROP is the subject of further experiments.

In summary, we have developed a facile Raman spectroscopic method to study enzyme-catalyzed ROP of lactones in real time. This *in situ* method allows rapid quantification of reactivity ratios and monomer conversion. We reported for the first time reactivity ratios for the enzyme-catalyzed copolymerization of  $\epsilon$ -CL and  $\delta$ -VL.

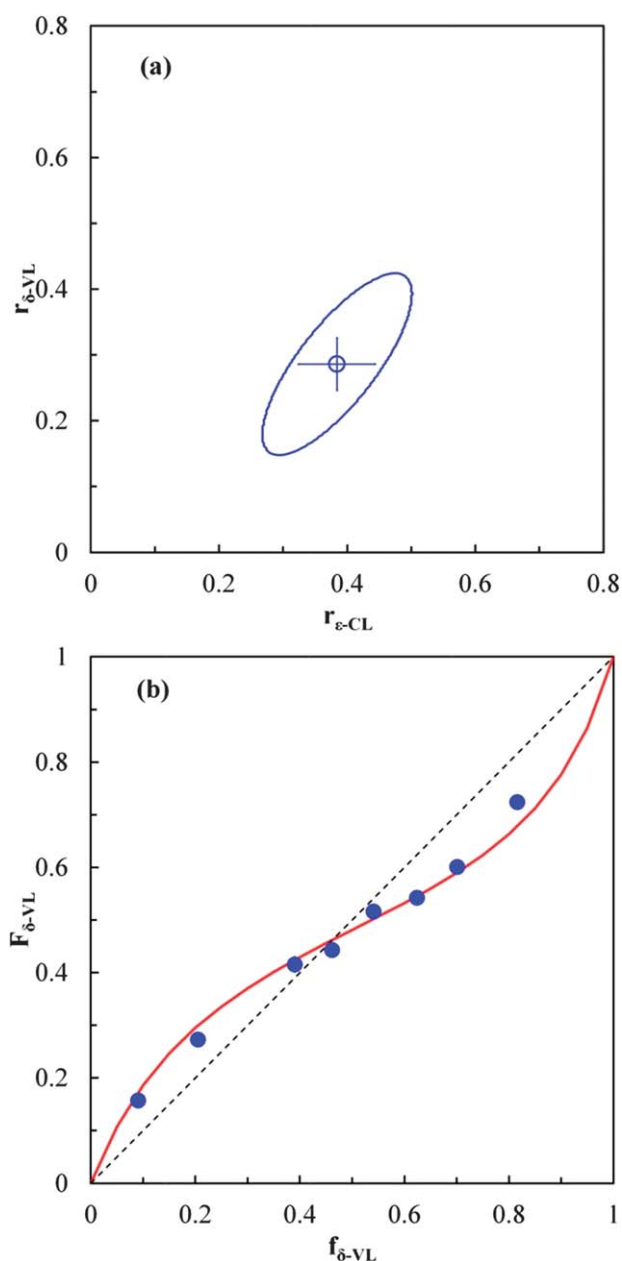


**Fig. 4** (a) The 95% joint confidence interval ellipse for monomer reactivity ratios determined using the K-T method. The point estimate reactivity ratios are shown as a circle and the error bars represent the standard error from the K-T analysis. (b) Copolymer composition as the fraction of  $\delta\text{-VL}$  in the copolymer ( $F_{\delta\text{-VL}}$ ) versus the fraction of  $\delta\text{-VL}$  in the monomer feed ( $f_{\delta\text{-VL}}$ ). The error bars (indicating one standard uncertainty based on measurements on at least three different samples) are smaller than the symbols. The solid line corresponds to eqn (4) with reactivity ratios  $r_{\epsilon\text{-CL}} = 0.39$  and  $r_{\delta\text{-VL}} = 0.29$ . The dashed line shows the case of  $r_{\epsilon\text{-CL}} = r_{\delta\text{-VL}} = 1$ .

Raman conversion and offline  $^1\text{H}$  NMR conversion produced equivalent conversion profiles of the ring-opening step of PCL polymerization and P(CL-co-VL) copolymerization. Raman spectroscopy has a number of benefits compared to traditional aliquot-based methods by eliminating problems associated with aliquot sampling and secondary offline analysis. The main advantage of the

Raman spectroscopic method was the ability to analyze kinetic rates at a variety of reaction conditions rapidly with a large number of data points over short time intervals. The technique is only limited by the ability to discriminate for a spectral peak associated with the reaction in question, and the flexibility of this technique would be attractive for implementation in both laboratory and industrial processes.

## Acknowledgements

The authors would like to thank Novozyme for providing the N435 beads. A.B. and R.G. thank the Industrial Members of the Biocatalysis Center at Polytechnic Institute of NYU for their financial support of this research. M.H. would like to acknowledge the support of the National Research Council Fellowship Program.

## Notes and references

- 1 A. Arbaoui and C. Redshaw, *Polym. Chem.*, 2010, **1**, 801–826.
- 2 M. K. Kiesewetter, E. J. Shin, J. L. Hedrick and R. M. Waymouth, *Macromolecules*, 2010, **43**, 2093–2107.
- 3 R. J. Pounder and A. P. Dove, *Polym. Chem.*, 2010, **1**, 260–271.
- 4 S. Kobayashi, *Macromol. Rapid Commun.*, 2009, **30**, 237–266.
- 5 O. Dechy-Cabaret, B. Martin-Vaca and D. Bourissou, *Chem. Rev.*, 2004, **104**, 6147–6176.
- 6 M. Tang, Y. Dong, M. M. Stevens and C. K. Williams, *Macromolecules*, 2010, **43**, 7556–7564.
- 7 S. Li, M. Pignol, F. Gasc and M. Vert, *Macromolecules*, 2004, **37**, 9798–9803.
- 8 J. Li, R. M. Stayshich and T. Y. Meyer, *J. Am. Chem. Soc.*, 2011, **133**, 6910–6913.
- 9 Z. Wei, L. Liu, C. Qu and M. Qi, *Polymer*, 2009, **50**, 1423–1429.
- 10 J. Wahlberg, P. V. Persson, T. Olsson, E. Hedenström and T. Iversen, *Biomacromolecules*, 2003, **4**, 1068–1071.
- 11 M. Van den Brink, W. Smulders, A. M. Van Herk and A. L. German, *J. Polym. Sci., Part A: Polym. Chem.*, 1999, **37**, 3804–3816.
- 12 A. J. Pasquale and T. E. Long, *J. Appl. Polym. Sci.*, 2004, **92**, 3240–3246.
- 13 K. A. George, F. Schué, T. V. Chirila and E. Wenstrup-Byrne, *J. Polym. Sci., Part A: Polym. Chem.*, 2009, **47**, 4736–4748.
- 14 J. H. Khan, F. Schué and G. A. George, *Polym. Int.*, 2010, **59**, 1506–1513.
- 15 B. Chen, J. Hu, E. M. Miller, W. Xie, M. Cai and R. A. Gross, *Biomacromolecules*, 2008, **9**, 463–471.
- 16 Y. Mei, A. Kumar and R. Gross, *Macromolecules*, 2003, **36**, 5530–5536.
- 17 Y. Mei, A. Kumar and R. A. Gross, *Macromolecules*, 2002, **35**, 5444–5448.
- 18 S. E. Barnes, Z. T. Cygan, J. K. Yates, K. L. Beers and E. J. Amis, *Analyst*, 2006, **131**, 1027–1033.
- 19 O. Elizalde, M. Azpeitia, M. M. Reis, J. M. Asua and J. R. Leiza, *Ind. Eng. Chem. Res.*, 2005, **44**, 7200–7207.
- 20 C. Murlì and Y. Song, *J. Phys. Chem. B*, 2010, **114**, 9744–9750.
- 21 S. Parnell, K. Min and M. Cakmak, *Polymer*, 2003, **44**, 5137–5144.
- 22 H. Dong, S.-G. Cao, Z.-Q. Li, S.-P. Han, D.-L. You and J.-C. Shen, *J. Polym. Sci., Part A: Polym. Chem.*, 1999, **37**, 1265–1275.
- 23 H. Uyama, K. Takeya and S. Kobayashi, *Proc. Jpn. Acad., Ser. B. Phys. Biol. Sci.*, 1993, **69**, 203–207.
- 24 F. Faÿ, E. Renard, V. Langlois, I. Linossier and K. Vallée-Rehel, *Eur. Polym. J.*, 2007, **43**, 4800–4813.
- 25 R. F. Storey and D. C. Hoffman, *Makromol. Chem., Macromol. Symp.*, 1991, **42–43**, 185–193.
- 26 N. Ropson, Ph. Dubois, R. Jerome and Ph. Teyssie, *Macromolecules*, 1994, **27**, 5950–5956.
- 27 A. López-Luna, J. L. Gallegos, M. Gimeno, E. Vivald-Lima and E. Bárzana, *J. Mol. Catal. B: Enzym.*, 2010, **67**, 143–149.
- 28 M. Fineman and S. D. Ross, *J. Polym. Sci.*, 1950, **5**, 259–262.
- 29 T. Kelen and F. Tudos, *J. Macromol. Sci. Chem.*, 1975, **A9**, 1–27.
- 30 D. L. Patton, K. A. Page, C. Xu, K. L. Genson, M. J. Fasolka and K. L. Beers, *Macromolecules*, 2007, **40**, 6017–6020.
- 31 R. K. Srivastava and A.-C. Albertsson, *Biomacromolecules*, 2006, **7**, 2531–2538.